UCRL-JC-124503
PREPRINT

Implementation and Performance of Beam Smoothing on 10 Beams of the Nova Laser

D. M. Pennington, S. N. Dixit, T. L. Weiland,
R. Ehrlich, and J. E. Rothenberg

This paper was prepared for submittal to
2nd Annual International Conference on Solid-State
Lasers for Applications to Inertial Confinement Fusion
Paris, France
October 22-25, 1996

March 11, 1997

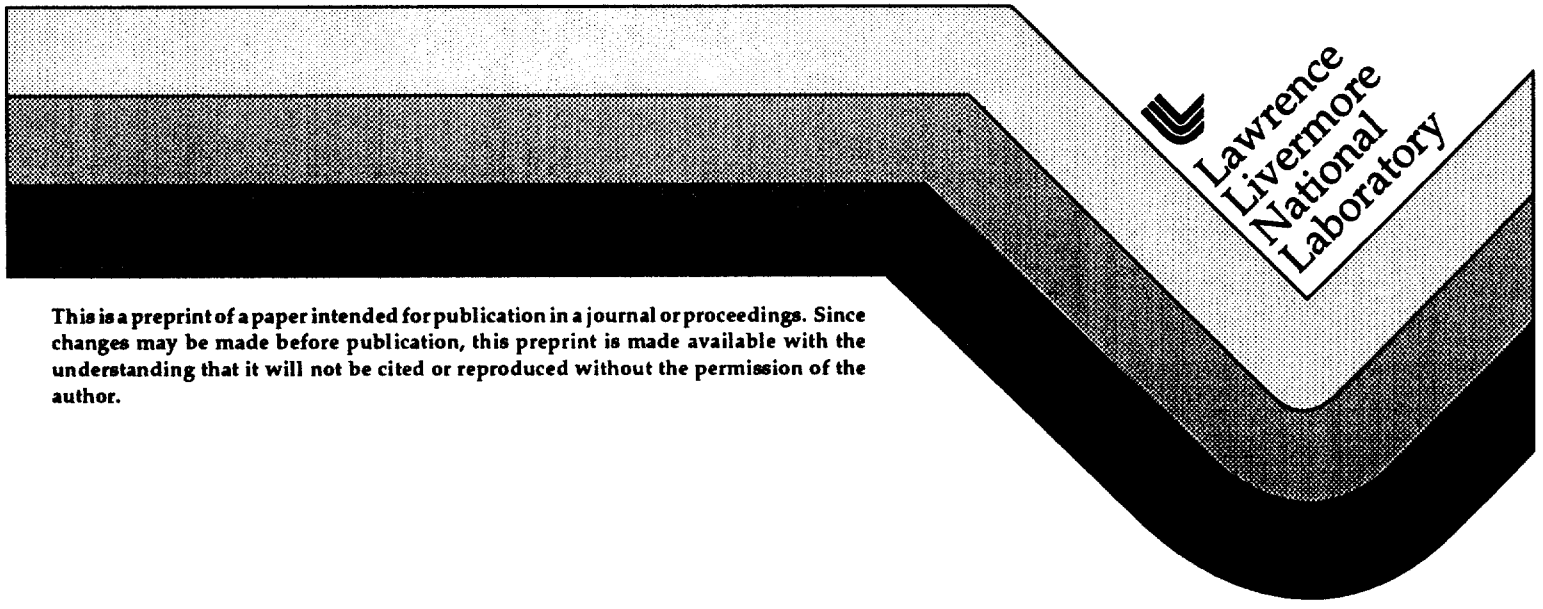

UCRL-JC-124503

IMPLEMENTATION AND PERFORMANCE OF BEAM SMOOTHING ON 10 BEAMS OF THE NOVA LASER

D. M. Pennington, S.N. Dixit, T.L. Weiland, R. Ehrlich, J.E. Rothenberg
Laser Program, Lawrence Livermore National Laboratory,
PO Box 808, L-439, Livermore, CA 94550
Telephone: (510) 423-9234, Telefax: (510) 422-5537
e-mail: pennington1@llnl.gov

ABSTRACT

Recent simulations and experiments on Nova indicate that some level of smoothing may be required to suppress filamentation in plasmas on the National Ignition Facility (NIF), resulting in the addition of 1-D smoothing capability to the current baseline design. Control of stimulated Brillouin scattering (SBS) and filamentation is considered essential to the success of laser fusion because they affect the amount and location of laser energy delivered to the x-ray conversion region (hohlraum wall) for indirect drive and to the absorptive region for direct drive. Smoothing by spectral dispersion (SSD)[1], reduces these instabilities by reducing nonuniformities in the focal irradiance when averaged over a finite time interval. We have installed SSD on Nova to produce beam smoothing on all 10 beam lines. A single dispersion grating is located in a position common to all 10 beam lines early in the preamplifier chain. This location limits the 1ω bandwidth to 2.2 Å with sufficient dispersion to displace the speckle field of each frequency component at the target plane by one half speckle diameter. Several beam lines were modified to allow orientation of the dispersion on each arm relative to the hohlraum wall. After conversion to the third harmonic the beam passes through a kinoform phase plate (KPP) designed to produce an elliptical spot at best focus. The KPPs produce a focal spot having an elliptical flat-top envelope with a superimposed speckle pattern. Over 93% of the energy is contained in the central 400 μm. Calculations indicate a 16 % rms. intensity variance will be reached after 330 ps for a single beam.

1.0 INTRODUCTION

Over the past few years optical smoothing of the laser irradiance on targets for inertial confinement fusion (ICF) has been given increasing attention.[1-8] Wave front aberrations in high power laser systems for ICF produce nonuniformities in the energy distribution of the focal spot that can significantly degrade the coupling of energy into a fusion target, driving various plasma instabilities. In particular, hot spots can induce local self-focusing of the light, producing filamentation of the plasma and beam deflection. Filamentation can have detrimental consequences on the hydrodynamics of an ICF plasma, and can affect the growth of parametric instabilities, as well as add to the complexity of the study of instabilities such as stimulated Brillouin scattering (SBS) and stimulated Raman scattering (SRS).[9-15]

The introduction of temporal and spatial incoherence to the beam, using techniques such as induced spatial incoherence (ISI)[2,3] or smoothing by spectral dispersion (SSD)[1], reduces intensity variations when averaged over a finite time interval. The SSD technique has been demonstrated on one beamline of the Nova laser at the second and third harmonic wavelengths, 527 and 351 nm, respectively,[4,6-8] and has been successfully used for target experiments[14,16-20]. Simulations indicate that SBS reflectivity increases due to filamentation, with a total gain greater than calculated for a uniform laser intensity. SBS reflectivities >10% may unacceptably degrade target performance by disrupting symmetry or reducing the energy available for radiation heating. Temporal smoothing makes filamentation less likely because the filament must form before the hot spot moves to a different location.

Initial target experiments with 10-B SSD will test the effects of beam smoothing on x-ray drive and radiation symmetry experiments in gas-filled hohlraums at NIF-relevant intensities. Previous experiments without beam smoothing showed that drive is reduced with high levels of SRS and SBS backscatter and

*Work performed under the auspices of the U.S. Department of Energy by the Lawrence Livermore National Laboratory under Contract W-7405-ENG-48.

Preliminary results indicate that a kinoform phase plate (KPP) alone reduces scattered light levels and improves radiation symmetry.[21]

1.1 Smoothing by spectral dispersion

Fig. 1 is a schematic of the SSD technique. Broadband light, produced in this case by electro-optic phase modulation (FM), is spectrally dispersed by a grating, and then amplified, frequency converted, and focused through a phase plate on to a target. Each distinct frequency component produces a speckle pattern, resulting in a superposition of many speckle patterns. Since each frequency propagates at a different angle through the phase plate, the speckle patterns spatially shift as a function of frequency. As the frequencies change throughout the length of the pulse, the rapidly fluctuating interference of the displaced speckle fields for the different spectral components causes the irradiance to appear smooth on a time-averaged basis. The most effective beam smoothing is when the speckle field for each spectral component is spatially shifted at the target plane one half the speckle diameter, $d_{1/2} = 1.22\lambda f/D$, where f is the focal length of the focus lens, λ is the third harmonic wavelength (3ω), and D is the diameter of the beam at the lens. [6] This condition, defined as critical dispersion, is often referred to as one color cycle since all FM frequencies are present when averaged across the lens. This level is achieved when the 3ω dispersion at the output aperture is fixed at $d\theta/d\nu = d_{1/2}/f \cdot \delta\nu$ in rad/Hz, for a specified spacing between spectral components, $\delta\nu$, and speckle size $d_{1/2}$.

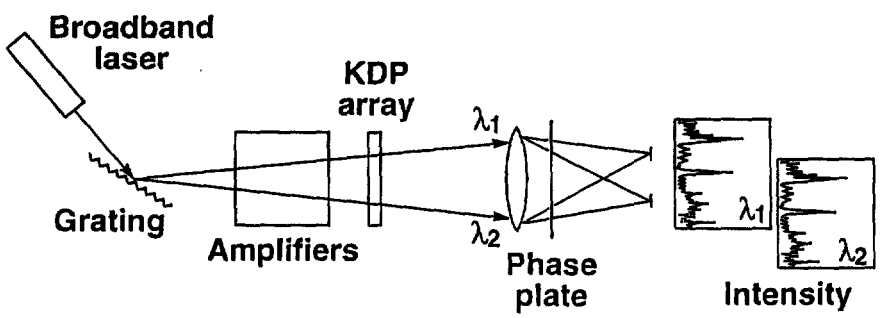

Fig. 1: Schematic diagram of the smoothing by spectral dispersion (SSD) method.

The time integrated smoothness, σ/I, is defined as the spatial rms. variance normalized to the average at the target plane. The smoothness is proportional to $1/\sqrt{n}$, where n is the number of decorrelated speckle fields superimposed at each point on the target. The effective time-integrated smoothing level for spectrally dispersed beams can be approximated by

$$\sigma / I \cong \sqrt{\tau \cdot \delta\nu} = \left[\frac{1.22\lambda}{\Delta\nu \cdot D} \left(\frac{d\theta}{d\nu} \right)^{-1} \right]^{1/2}, \qquad (1)$$

where $\delta\nu$ is the effective separation between independent spectral components in Hz, τ is the coherence time in seconds, $\Delta\nu$ is the frequency converted bandwidth in GHz, and $d\theta/d\nu$ is the grating dispersion at 3ω in rad/Hz. For critical dispersion, ν is the total number of spectral components in the beam and $d\nu$ is the modulation frequency of the electro-optic phase modulator. Instantaneously, $\sigma/I \equiv 1$ due to basic Rayleigh speckle statistics, but this value decreases rapidly as the irradiance variations are varied over time. The initial smoothing occurs on a time scale proportional to $1/\tau$, reaching an asymptotic value given by Eq. (1) in a time determined by $1/\delta\nu$. The initial onset of smoothing is delayed due to the spatially varying time delay across the beam imposed by the grating (i.e., a delay of λ/c per illuminated grating line). This time delay τ_d is proportional to $1/\delta\nu$, and therefore n is proportional to τ_d/τ.

1.2 10-Beam SSD Design Criteria

Recent experiments on Nova, and simulations by Berger et. al.[22,23] provided the design criteria for 10-B SSD. The principle conclusions from these simulations were (1) that critically dispersed SSD with ~ 3Å bandwidth (before frequency conversion) should be sufficient to control beam deflection and filamentation with flow, (2) that multiple color cycles have little benefit on beam deflection or filamentation beyond that obtained with one-color cycle at the same bandwidth, (3) that the orientation of the SSD dispersion direction across transverse flow direction is advantageous for suppression of filamentation, but has a small effect on beam deflection suppression, and (4) that, on time scales short compared to an FM color cycle, SSD itself leads to "beam deflection". This particular effect time averages away over the period of an FM color cycle. Most of these effects are mitigated by producing a given bandwidth with higher FM modulation frequency and smaller modulation depth. This decreases the required dispersion, which produces a less distorted spot in the laser entrance hole (LEH) of the hohlraum. Further calculations indicate that a minimum of 1.25 Å must be used to affect filamentation, and that 5 Å or greater is optimal.

The achievable dispersion/bandwidth product is determined by the angular acceptance of the laser chain. The level of obtainable smoothing is a trade off between bandwidth and dispersion. The initial rate of smoothing is proportional to the bandwidth; however, to achieve efficient third harmonic conversion, the allowable bandwidth should not exceed the phase matching tolerance of the conversion crystals. In order to remain within 10% of the maximum conversion efficiency, the input bandwidth should be limited to ~ 2 Å.[7,24] The second limitation, angular acceptance of the laser chain, also impact the choice of bandwidth. For our conditions, this constraint limits the allowable bandwidth to 2.2 Å with critical dispersion for the modulation frequency available (3 GHz). The dispersion direction can be oriented either azimuthally or axially in the hohlraum by changing the grating mounting configuration. The expected smoothing performance as a function of bandwidth for a 3 GHz modulator with critical dispersion is shown in Fig. 2. Calculations indicate a 26 % rms. intensity variance (σ/I) will be reached after 50 ps for a single beam, reducing to 16% after 330 ps.

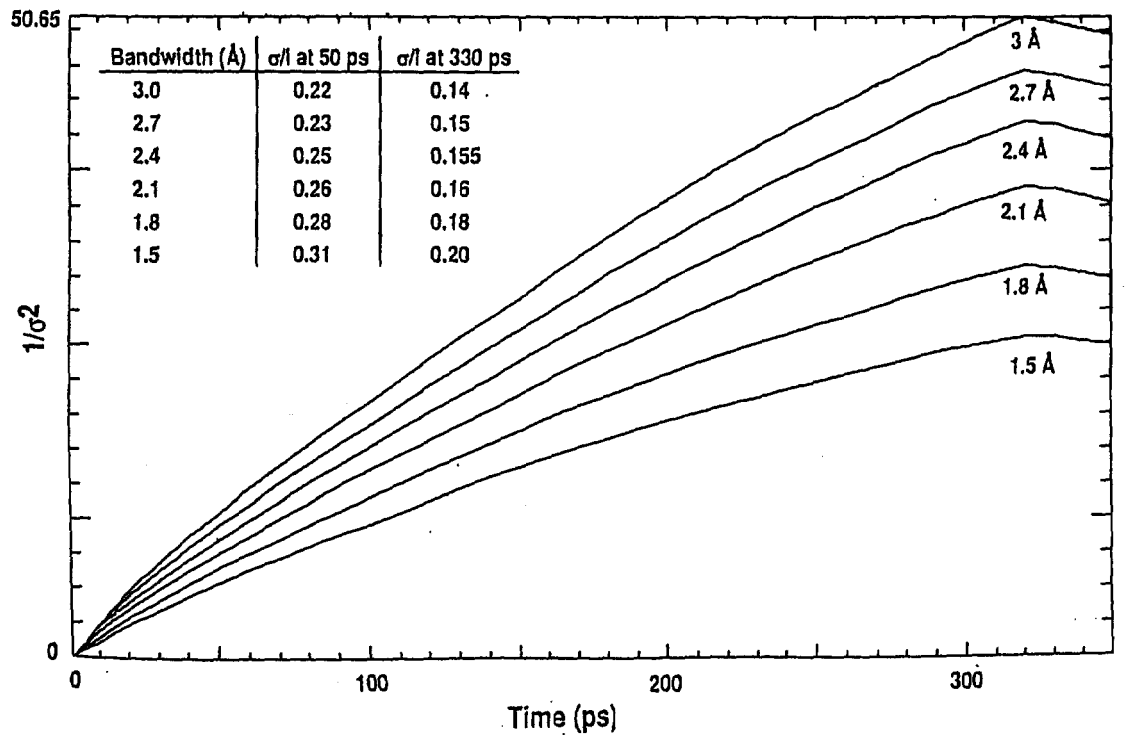

Bandwidth (Å)	σ/I at 50 ps	σ/I at 330 ps
3.0	0.22	0.14
2.7	0.23	0.15
2.4	0.25	0.155
2.1	0.26	0.16
1.8	0.28	0.18
1.5	0.31	0.20

Fig. 2: The expected smoothing performance as a function of bandwidth for a 3 GHz modulator with critical dispersion; σ is the rms. intensity variance.

2.0 EXPERIMENTAL DESIGN AND IMPLEMENTATION

2.1 Bandwidth Source

Bandwidth for SSD is added immediately following the pulse shaping system in the MOR, by passing the beam through an electro-optic phase modulator. The effect is to produce a laser electric field of the form

$$E(t) = E_0 \exp(i\omega t + i\delta \sin \omega_m t) \quad , \tag{2}$$

where δ and ω_m are the modulation amplitude and angular frequency of the electro-optic device, and ω is the fundamental angular frequency of the laser. Expanding this in a Fourier series,

$$E(t) = E_0 \sum J_n(\delta) \exp(i\omega t + in\omega_m t) \quad , \tag{3}$$

we see that the beam contains side bands in increments of ω_m, which extend out to approximately $\pm\ \delta\omega_m$, at which point the frequency spread is well approximated by $\Delta\nu = 2\delta\nu_m$, in terms of the modulation amplitude and frequency. The beam was propagated through a double-passed electro-optic phase modulator, consisting of a $LiNbO_3$ crystal in a microwave cavity modulated at 3 GHz, obtained from the Laboratory for Laser Energetics at the University of Rochester. This device allowed the addition of 2.2 Å of bandwidth when the device was turned on to provide SSD. There was no effect due to this device when it was turned off. Application of FM bandwidth imposes a 7-15% peak-to-peak amplitude modulation on the 1ω beam at 3 GHz.

2.2 Implementation

Several design modifications were required to implement SSD on all 10 Nova beamlines. It is noteworthy that most of these modifications are common to the implementation of beam phasing on Nova. [25] The most cost effective method to implement dispersion on all 10 arms is to use a single grating. This requires that the dispersion be applied before the 2-way split in the laser pre-amplifier chain, as shown in Fig. 3. A large optical table was installed in the Nova pre-amplifier section to hold the SSD grating and associated optics. The beam is injected onto this table with kinematic mirrors to allow a quick return to the standard pre-amplifier configuration. An optical relay on the table images the grating to the next image plane in the amplifier chain. Propagation through the SSD table adds the equivalent of 36 ns to the total path beam path. An 4 ns delay is also added on each arm due to the addition of beam rotation modules and optical delay lines described below, for a total beam path delay of 40 ns. To avoid re-timing the target diagnostics, we compensated for the added delay by switching a later pulse out of the timing oscillator pulse train and adjusting an optical delay line on the SSD table.

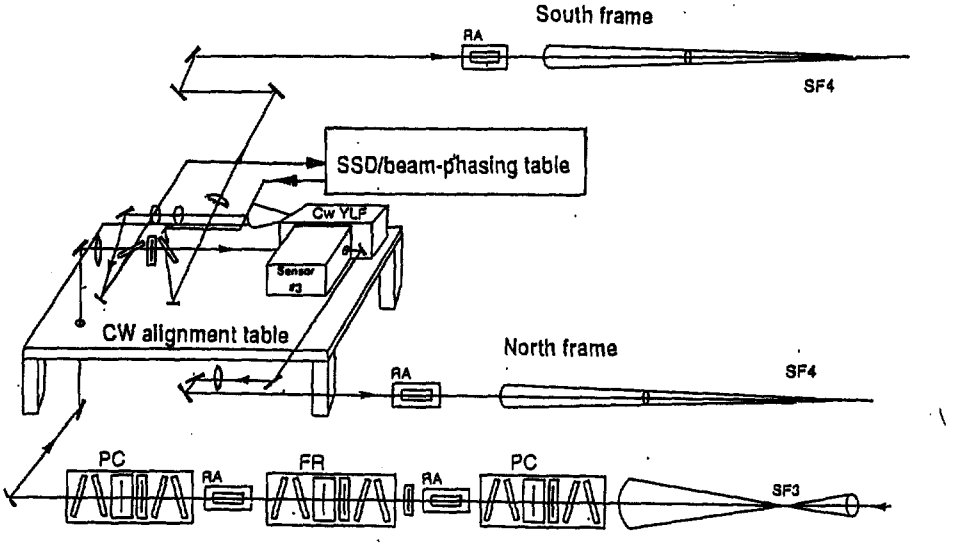

Fig. 3: The 10-B SSD grating is located in the pre-amplifier section before the 2-way beam split, making it common to all 10 beams.

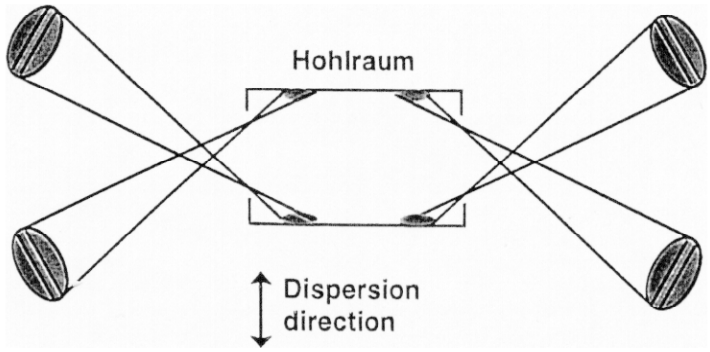

Fig. 4: Symmetric target irradiation requires that the orientation of the dispersion be the same for each beam at target chamber center. The dispersion can be oriented either axially or azimuthally along the hohlraum wall by changing the grating orientation.

Symmetric target irradiation requires that the orientation of the dispersion be the same for each beam at target chamber center, as shown in Fig. 4. Setting the dispersion direction either along or perpendicular to hohlraum axis is accomplished by changing the grating dispersion orientation from horizontal to vertical on the SSD table, and adding a quartz polarization rotator. This is sufficient to orient six of the beams correctly inside a hohlraum. However, beams 3, 4, 7, and 8 are rotated by 45° upon reaching the target, as shown in Fig. 5. Optical rotation modules, composed of a 22.5° out of plane delay leg, were installed to re-orient these beams. This added 4 ns delay to each of these beams. The insert mirrors in each rotation module are kinematic to allow quick return to normal operations. In addition, the optical delay lines on the other six beams were extended by 4 ns to compensate for the increase in path length due to the rotation modules. These extensions allow precision timing of all 10 beams on target.

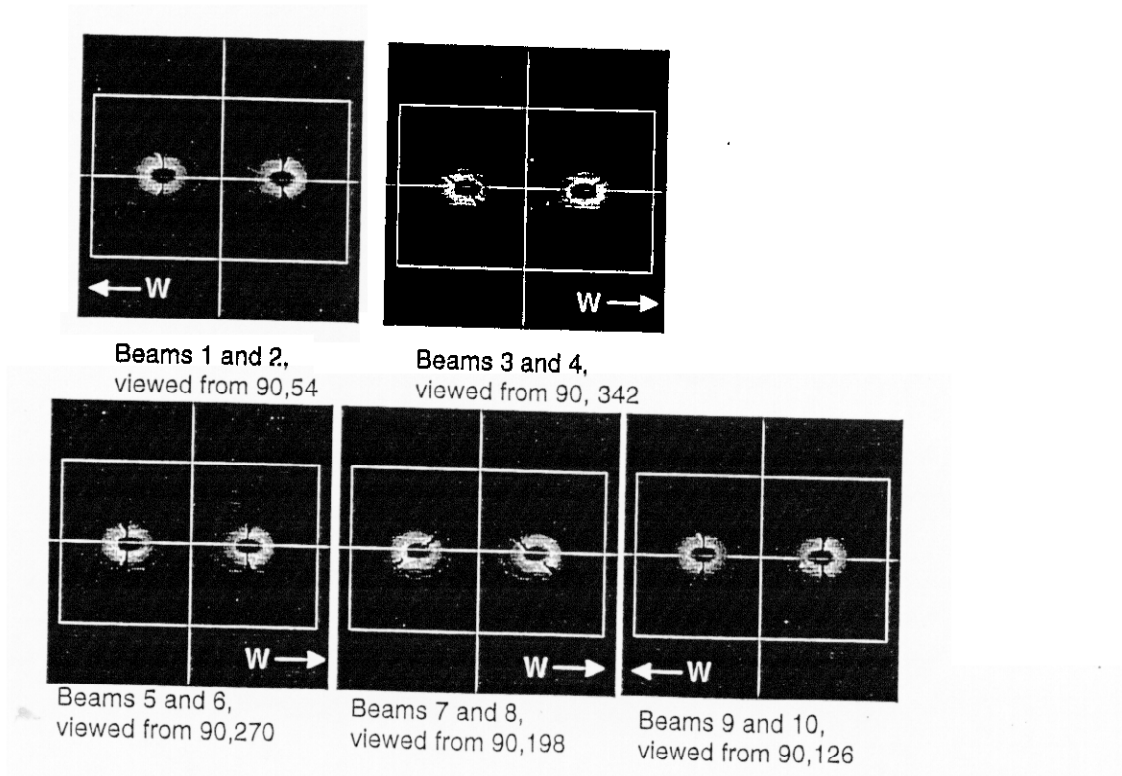

Fig.5: Simulation of the 2 beam orientations inside a hohlraum without beam rotation modules.

The standard relaying in the Nova pre-amplifier section is insufficient both for SSD and beam phasing. In the case of SSD, the grating must be properly relayed through the amplifier chain to avoid amplitude

modulation. The peak-to-peak amplitude modulation incurred by unrelayed propagation of a beam with FM bandwidth can be calculated by the following relation:

$$\%\text{peak} - \text{to} - \text{peak AM} \approx (z\beta N_c^2 / 5D^2), \tag{4}$$

where, z is the propagation distance from a relay plane (cm), $\beta \sim \Delta\nu/2\nu_{mod}$ FM is the modulation depth, D is the beam diameter (cm), $\Delta\nu$ is the bandwidth (GHz), ν_{mod} is the modulation frequency (GHz), and N_c is the number of color cycles. The current pre-amplifier relay system throws the serrated aperture image to an average distance for ten arms. This distance can vary up to15.85 m from arm to arm. Figure 6 shows the modulation incurred by propagating the beam 10 m unrelayed from the 10-B SSD grating location. Relay optics were added to relay the SSD grating through the pre-amplifier section common to all 10 beams. With these optics in place, beams 3, 4, 7 and 8, all of which require rotation modules, were sufficiently relayed. The other six beams required installation of additional relaying in each arm. Based on the performance of single beam SSD with the FM modulator on Nova, where the grating is relayed through the chain, we expect 7-15% peak-to-peak modulation on the beam with the proper relaying. This is consistent with the modulation observed at the output of the FM modulator in the MOR. [7,8] This is an acceptable modulation level for propagation through the chain, and should have less than a 5 - 10% effect on 3ω conversion efficiency.

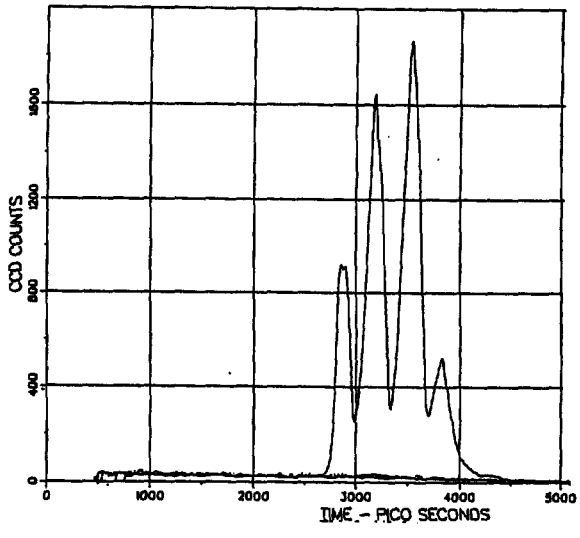

Fig.6: Amplitude modulation incurred by propagating the beam 10 m unrelayed from the 10-B SSD grating location.

2.3 Bandwidth/Dispersion Optimization

In this location, a 1730 gr./mm grating is required to provide critical dispersion in the target plane. With a 3 GHz modulator, the modulation period is $T = 1/\Delta\nu = 333$ ps. To achieve critical dispersion for a circular beam requires a grating delay of $\tau_d = 1.22$ (333 ps) = 406 ps. This delay corresponds to $d\theta/d\lambda = c\tau_d/\lambda D = 16.52$ μrad/Å at 1ω at the output of the laser chain. Accounting for the chain magnification, this requires a 441 ps delay at the SSD grating. The grating is located before the defining 23-mm serrated aperture for the laser chain. Under normal operating conditions the aperture would reduce the time delay by a factor of 0.72. To compensate for this effect, we operate the grating several degrees off Littrow, and allow the associated compression of the beam along the axis of dispersion to under fill the aperture in one dimension. A beam diameter of 25 mm was chosen along the dispersion axis to allow some spatial tailoring of the edges of the beam profile. Operation of the grating in a non-Littrow configuration changes the grating time delay a dispersion somewhat. We solve 3 simultaneous equations to obtain the optimal diffraction angles :

$$\sin\theta_{in} + \sin\theta_{out} = m\lambda / d$$
$$D_{out} / D_{in} = \cos\theta_{out} / \cos\theta_{in} \qquad (5)$$
$$\tau_d = \lambda D_{out} / (cd \cos\theta_{out}).$$

The solution for τ_d = 441 ps, $1/d$ = 1730 gr./mm, λ = 1053 nm, D_{in} = 34 mm, and D_{out} = 25 mm, θ_{in} = 62°, θ_{out} = 69.8° and $d\theta/d\lambda$ = 501 μrad/Å.

The maximum dispersed bandwidth that can be propagated through the laser chain is determined by the angular acceptance of the spatial filter pinholes following the SSD grating. To maximize the angular acceptance of the limiting components in the preamplifier, SF-4 and SF-5, we increased the pinhole diameter from 8 to 12 mm, and opened up the interior light baffles. Since the only active component between SF4 and the next spatial filter, SF1, is a Pockels cell, SF-1 provides sufficient isolation for the chain. The new angular acceptance of SF-4 with a ± 10% alignment tolerance is $\Delta\lambda(d\theta/d\lambda)$ = 1.11 mrad full angle. All other spatial filter pinholes following SF-4 and SF-5 were set to the largest pinhole setting (20X diffraction limit). This sets the maximum allowable bandwidth at 2.2 Å, which is consistent with the phase-matching tolerance for efficient 3ω conversion.

2.4 KPP Design

A kinoform phase plate (KPP) was designed to produce a spot with a NIF single beam intensity of 2 x 10^{15} W/cm^2 with SSD for a 2 TW Nova beam power, as shown in Fig. 7.[26] An F/4.3 focal geometry was assumed. The design also incorporates the flexibility to vary the bandwidth and dispersion direction to produce a round spot, ~10^5 μm^2, without the beam spreading associated with SSD. The spot area at best focus is given by πab, where a is the radius in the azimuthal direction and b is the spot radius in the direction which projects axially on the hohlraum wall. The increase in diameter, Δa, due to dispersion along a is ~ 52 μm per 1 Å of 1ω. To produce a round spot in the LEH requires that $b = (a \cos(50°) + \Delta a/2)$, giving a ~ 204 μm and b ~ 131 μm for 2.2 Å 1ω FM bandwidth.

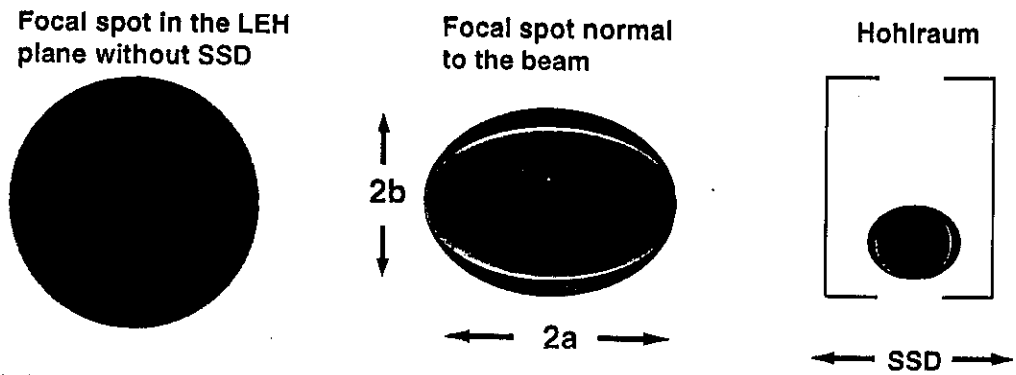

Fig. 7: A kinoform phase plate (KPP) was designed to produce a spot with a NIF single beam intensity of 2 x 10^{15} W/cm^2 with 2.2 Å of bandwidth and SSD for a 2 TW Nova beam power.

2.3 System Flexibility And Limitations

When in place, the 10-B SSD configuration places limits on certain Nova systems. Addition of the SSD grating places a time delay on the beam that affects the integrated temporal pulse shape. Experiments requiring a sharp rising edge for timing purposes are particularly sensitive to this affect. Temporally pre-skewing the beam is not practical on Nova due limiting apertures early in the laser chain. Relocation of the FM modulator to the SSD grating table would allow pre-correction, and the potential to implement 2-D SSD with the addition of a second high frequency modulator in the MOR. Backlighter capability is limited with SSD. Beams 3, 7, and 8 are still available as backlighters with an independent pulse shape, however, backlighter delays are limited in order to maintain the new image relaying. Approximately 3% amplitude modulation per 1 ns of delay would be incurred. Precision power balance will be used on the first 10-B SSD target shots. Precision power balance requires the addition of different size beam defining apertures on each beamline to achieve the same power out of all arms. Those apertures smaller than the standard size will remove a portion of the SSD time delay, reducing the dispersion below the critical

level. We estimate the apertures will remove at most 10% of the time skew. Simulations of the smoothing performance with 90% of a color cycle indicate this has ~10% effect on the asymptotic smoothing level, and that there is little effect on the smoothing rate until greater than 60 ps. The bandwidth remains the same since the apertures are placed in the near field.

3.0 ACTIVATION AND PERFORMANCE

Activation of 10-B SSD began with low power propagated rod shots to the Nova output sensor, in order to time each of the new delay lines to the desired position. This brought the beam timing to within ~ 100 ps of each other. Timing was determined for the standard Nova and backlighter configurations with and without the rotation modules and relaying, and with and without the SSD path. To synchronize the arrival of all ten beams on target to within 50 ps, a gold disk target was illuminated by the pulses from all 10 Nova beams.[27] A 180 ps pulse was propagated on all of the arms. The odd and even beams were aligned to produce interleaved spots on the east and west sides of the target, respectively. The time-dependence of the x-ray emission was monitored by streak cameras that view the target edge-on from the north and south. Adjustments to beam timing were then made by varying the length of the optical delays installed in each arm with a rotation module.

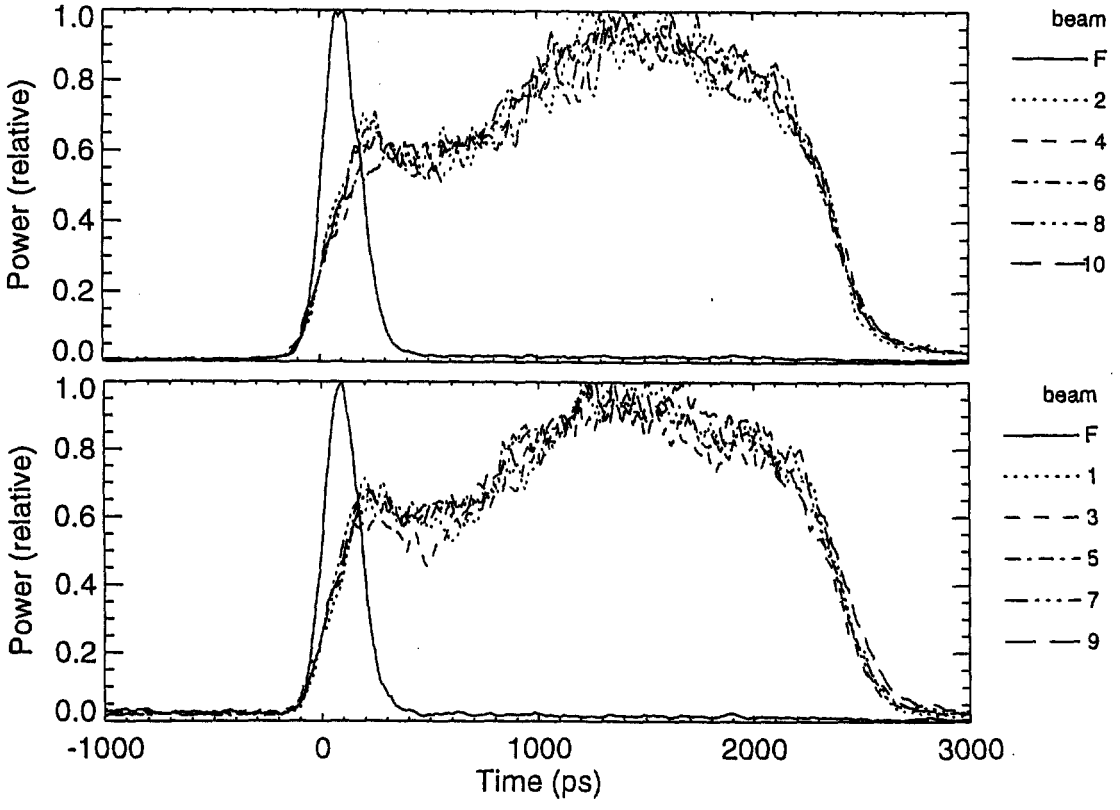

Fig. 8: Temporal profiles demonstrate it is possible to obtain output pulses at full power with 10-B SSD with as little as ± 7% temporal modulation.

Temporal profiles were recorded both with LLNL streak cameras and fast photodiodes to measure the amplitude modulation with the new relaying. In addition, near field beam images were carefully monitored for evidence of small-scale self-focusing. The streak camera profiles shown in Fig. 8 demonstrate it is possible to obtain output pulses at full power with as little as ± 5% temporal modulation. Several shots were taken with increasing output energy until > 10 kJ 1ω was achieved. A 2.2 ns ramped pulse shape was used. Third harmonic frequency conversion with this pulse shape is typically ~ 30 - 35%. The addition of SSD affected the conversion efficiency by < 5%, as expected. The near field beam

images indicated the system was close to the self-focusing threshold at >10 kJ output, in particular on the arms that showed > 10% temporal modulation. Even with the 20% alignment tolerance through the spatial filter pinholes, extreme care is required to avoid pinhole clipping. The pinholes require manual alignment as close to the system shot as possible to avoid alignment drift. It was also noted that clipping occurred most frequently on system shots, indicating that pump induced distortions contribute to misalignment of the beam through the pinholes. Since SF-4 and SF-5 are the tightest apertures in the system, they have the most critical alignment tolerance. Clipping in these pinholes can cause up to ± 30 % modulation, and has a dramatic affect on the preamplifier gain. Fortunately, this can be diagnosed on rod shots, and corrected for the system shot. While the amplitude modulation generated by clipping is still within the acceptable operational limit, the pulse shape distortion may be unacceptable for the target interactions. The reduction in power associated with this clipping was on the 1% level, indicating that we should be able reduce the alignment sensitivity and amplitude modulation by limiting the FM bandwidth to ~ 2 Å.

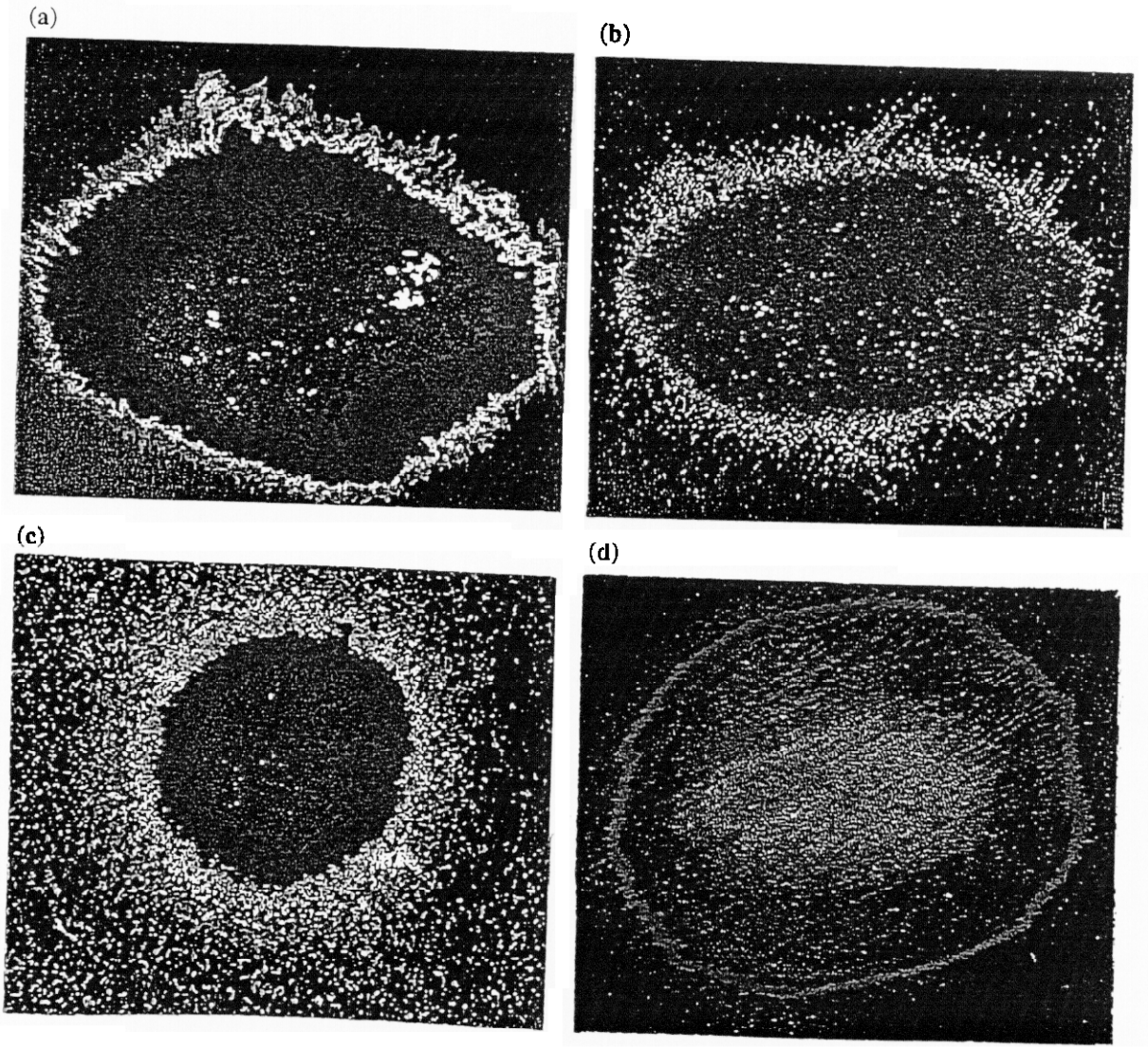

Fig. 9: (a) Equivalent target plane image taken with a single frequency beam at 3ω with a KPP, approximately 200 μm from best focus. (b) Simulated best focus spot for image shown in (a). (c) X-ray emission image taken at best focus in the plane of the LEH show a flat top circular beam, consistent with KPP design specifications. (d) Equivalent target plane image with 2.2 Å (1ω) of FM bandwidth and SSD taken at 3ω approximately 200 μm from best focus.

The focal spot of an unsmoothed single frequency beam shows significant structure due to laser system aberrations and beam obscurations in the near field. Figure 9(a) shows an equivalent target plane image taken with a single frequency beam at 3ω with a KPP, approximately 200 μm from best focus. At normal incidence, ~ 93% of the energy is within a 450 μm circle. This image is in good agreement with the simulated best focus spot shown in 9(b). The beam structure with the KPP is broken up into a homogeneous well-controlled speckle pattern with σ/I = 0.45. This deviates from theoretical prediction of σ/I = 1.0. Previous experiments on Nova[7] and elsewhere[28] have reported σ/I < 1 for images with random phase plates. Our previous measurements of a random phase plate taken in the same diagnostic used in these experiments produced σ/I ~ 0.8 for several random phase plates. Some of the increased smoothness may be due to chromatic and polarization smoothing occurring due to the birefringence in the focus lens, as well as resolution in the diagnostic and data. The additional deviation from theory is currently under investigation. An x-ray emission image taken at best focus in the plane of the LEH shows a flat-top circular beam consistent with design specifications (Fig. 9(c)).[21] The time integrated equivalent plane image at 3ω with 2.2 Å (1ω) of FM bandwidth and SSD is shown in Fig 9(d). The image shows the streaks characteristic of 1-dimensional SSD, with σ/I = 0.18 integrated over 2.2 ns, consistent with theoretical expectations.

4.0 SUMMARY

Beam smoothing has now been activated on all 10 Nova beamlines. The dispersion can be oriented either axially or azimuthally along the hohlraum wall by changing the grating orientation. Appropriate relaying in the amplifier chain allows the propagation of full power beams with as little as ± 5% temporal amplitude modulation due to FM bandwidth and SSD. Kinoform phase plates (KPP) were designed and fabricated to produce a spot with a NIF single beam intensity of 2 x 10^{15} W/cm^2 for a 2 TW Nova beam power, with 2.2 Å of bandwidth and critical dispersion. Equivalent target plane images taken at normal incidence with a single frequency beam at 3ω with a KPP, demonstrate ~ 93% of the energy is within a 450 mm circle. The equivalent target plane image taken at 3ω with 2.2 Å (1ω) of FM bandwidth and critical dispersion is quite smooth, with σ/I = 0.18 integrated over 2.2 ns.

5.0 ACKNOWLEDGEMENTS

The authors would like to acknowledge D. Kalantar, G. Glendinning, and B. Hammel for technical discussions and assistance, M. Rushford for KPP fabrication, K. Moffitt and R. Horton for design work, J. Peterson and R. Luthi for assistance with activation of 10-B SSD, and the members of the Nova Engineering and Operations staff for their overall support of the activation and performance of experiments.

6.0 REFERENCES

[1] S. Skupsky, R. W. Short, T. Kessler, R. S. Craxton, S. Letzring, and J. M. Soures, *J. Appl. Phys.*, vol. 66, pp. 3456-3462, 1989.

[2] R. H. Lehmberg and S. P. Obenschain, *Opt. Comm.* , vol. 46, pp. 27, 1983.

[3] S. P. Obenschain, J. Grun, M. J. Herbst, K. J. Kearney, C. K. Manka, E. A. McLean, *et. al.*, *Phys. Rev. Lett.* , vol. 56, pp. 2807, 1986.

[4] H. T. Powell, S. N. Dixit, and M. A. Henesian, *ICF Quarterly Report, Lawrence Livermore, National Laboratory, Livermore,CA, UCRL-LR-105821-91-1*, pp. 28-38, 1991.

[5] P. H. Chaffee, F. G. Patterson, and M. A. Henesian, *"Technical Digest, Conference on Lasers and Electro-Optics* , vol. 10, pp. 106, 1989, Optical Society of America, Anaheim, CA.

[6] M. A. Henesian, S. N. Dixit, H. T. Powell, C. E. Thompson, P. J. Wegner, and T. L. Weiland, *IQEC Technical Digest* , vol. 9, paper TuE3, 1992.

[7] D. M. Pennington, M. A. Henesian, S. N. Dixit, H. T. Powell, C. E. Thompson, and T. L. Weiland, *Proc. Soc. Photo-Instrum. Eng.* , vol. 1870, pp. 175-185, 1993.

[8] D. M. Pennington, M. A. Henesian, R. B. Wilcox, T. L. Weiland, and D. Eimerl, *ICF Quarterly Report, Lawrence Livermore National Laboratory, Livermore, CA, UCRL-LR-105820-95-2*, pp. 130-141, 1996.

[9] W. L. Kruer, *The Physics of Laser Plasma Interactions* . New York: Addison-Wesley, 1988.

[10] J. F. Drake, P. K. Kaw, Y. C. Lee, G. Schmidt, C. S. Liu, and M. N. Rosenbluth, *Phys. Fluids* , vol. 17, pp. 1778, 1974.

[11] R. L. Berger, *Phys. Rev. Lett.* , vol. 65, pp. 1207-1210, 1990.

[12] W. Seka, R. E. Bahr, R. W. Short, A. Simon, R. S. Craxton, D. S. Montgomery, and A. E. Rubenchik, *Phys. Fluids B* , vol. 4, pp. 2232-2240, 1992.

[13] R. L. McCrory, J. M. Soures, C. P. Verdon, F. J. Marshall, S. A. Letzring, T. J. Kessler, *et. al, Laser Part. Beams* , vol. 8, pp. 27-32, 1990.

[14] L. V. Powers, R. E. Turner, R. L. Kauffman, R. L. Berger, P. Amendt, C. A. Back, *et. al. Phys. Rev. Lett.*, vol. 74, pp. 2957-2960, 1994.

[15] R. L. Berger, T. B. Kaiser, B. F. Lasinski, C. W. Still, A. B. Langdon, S. N. Dixit, D. Eimerl, and D. M. Pennington, *ICF Quarterly Report, Lawrence Livermore, National Laboratory, Livermore,CA, UCRL-LR-105820-95-3*, pp. 200-207, 1996.

[16] S. G. Glendinning, S. V. Weber, P. Bell, L. B. DaSilva, S. N. Dixit, M. A. Henesian, *et. al., Phys. Rev. Lett.* , vol. 69, pp. 1201-1204, 1992.

[17] J. D. Moody, H. A. Baldis, D. S. Montgomery, C. Labaune, R. L. Berger, S. Dixit, *et. al. Bull. Am. Phys. Soc.* , vol. 37, pp. 1441, 1992.

[18] D. S. Montgomery, H. A. Baldis, J. D. Moody, R. L. Berger, K. G. Estabrook, E. A. Williams, and C. Labaune, *Bull. Am. Phys. Soc.* , vol. 37, pp. 1441, 1992.

[19] S. G. Glendinning, S. V. Weber, S. N. Dixit, M. A. Henesian, J. D. Kilkenny, D. M. Pennington, *et. al.*," *Anomalous Absorption Conference, Pacific Grove, CA June 5-10, 1994* , pp. DO-1, 1994.

[20] B. MacGowan, R. Berger, J. Frenandez, B. Afeyan, C. Back, G. Bonnaud, M. Casanova, *et. al., ICF Quarterly Report, Lawrence Livermore, National Laboratory, Livermore,CA, UCRL-LR-105820-95-4*, pp. 305-332, 1996.

[21] R. L. Kauffman, L. V. Powers, S. G. Glendinning, T. Orzechowski, L. J. Suter, R. L. Berger, *et. al.* , "Effects of beam conditioning on gas-filled hohlraum performance," presented at Annual Meeting of the American Physical Society, Plasma Physics Division, 1996.

[22] D. Berger, D. Hinkle, B. Langdon, B. Still, and E. Williams, "Beam smoothing requirements for NIF deduced from F3D simulations of filamentation," internal memo,LLNL,X96-009, 1/29/96.

[23] D. E. Hinkle, E. A. Williams, R. L. Berger, and A. B. Langdon, "Filamentation and beam deflection dependence on SSD bandwidth and number of color cycles," internal memo, LLNL X96-070, 5/3/96.

[24] M. D. Skeldon, R. S. Craxton, T. J. Kessler, W. Seka, R. W. Short, S. Skupsky, and J. M. Soures, *IEEE J. Quantum Electron.*, vol. 28, pp. 1389-1399, 1992.

[25] R. B. Ehrlich, P. A. Amendt, S. N. Dixit, B. A. Hammel, D. H. Kalantar, D. M. Pennington, and T. L. Weiland, "Developing beam phasing on the Nova laser," presented at Solid-State Lasers for Application to Inertial Confinement Fusion, Paris, France, 1996.

[26] M. C. Rushford, S. N. Dixit, I. M. Thomas, A. M. Martin, and M. D. Perry, "Large aperture kinoform phase plates in fused silica for spatial beam smoothing on Nova and the Beamlet lasers," presented at Solid-State Lasers for Application to Inertial Confinement Fusion, Paris, France, 1996.

[27] O. L. Landen, et.al., ," *Rev. Sci. Instr.* , vol. 66, pp. 788-790, 1995.

[28] T. Jitsuno and N. Nishi, "personal communication," , May 16, 1994.